# Thermodynamics of Ligand Binding and Catalysis in Human Liver Medium-Chain Acyl-CoA Dehydrogenase: Comparative Studies Involving Normal and 3′-Dephosphorylated $C_8$-CoAs and Wild-Type and Asn191 → Ala (N191A) Mutant Enzymes†

Kevin L. Peterson, Karen M. Peterson, and D. K. Srivastava*

*Biochemistry Department, North Dakota State University, Fargo, North Dakota 58105*

*Received April 27, 1998; Revised Manuscript Received June 22, 1998*

ABSTRACT: Following our demonstration that the terminal 3′-phosphate group of acyl-CoA substrates (which is confined to the exterior of the protein structure, and is fully exposed to the outside solvent environment) exhibits a functional role in the recombinant human liver medium-chain acyl-CoA dehydrogenase (MCAD)-catalyzed reaction [Peterson, K. L., and Srivastava, D. K. (1997) *Biochem. J. 325*, 751−760], we became interested in delineating its thermodynamic contribution in stabilizing the "ground" and "transition" state structures during enzyme catalysis. Since the 3′-phosphate group of the coenzyme A thiolester has the potential to form a hydrogen bond with the side chain group of Asn-191, these studies were performed utilizing both normal and 3′-dephosphorylated forms of octanoyl-CoA and octenoyl-CoA (cumulatively referred to as $C_8$-CoA) as the physiological substrate and product of the enzyme, respectively, as well as utilizing wild-type and Asn191 → Ala (N191A) site-specific mutant enzymes. The experimental data revealed that the enthalpic contribution of the 3′-phosphate group was similar in both ground and transition states, and was primarily derived from the London−van der Waals interactions (between the 3′-phosphate group of $C_8$-CoA and the surrounding protein moiety), rather than from the potential hydrogen bonding. The temperature dependence of $\Delta H°$ for the binding of octenoyl-CoA and 3′-dephosphooctenoyl-CoA revealed that the deletion of the 3′-phosphate group from octenoyl-CoA increased the magnitude of the heat capacity changes ($\Delta C_p°$) from −0.53 to −0.59 kcal mol$^{-1}$ K$^{-1}$. Although the latter effect could be attributed to an increase in the relative hydrophobicity of the ligand, the experimentally observed $\Delta C_p°$'s (for either of the ligands) could not be predicted on the basis of the changes in the solvent-accessible surface areas of the enzyme and ligand species. These coupled with the fact that the $\Delta C_p°$ for the binding of octenoyl-CoA to pig kidney MCAD (which is believed to be structurally identical to human liver MCAD) is only −0.37 kcal mol$^{-1}$ K$^{-1}$ [Srivastava, D. K., Wang, S., and Peterson, K. L. (1997) *Biochemistry 36*, 6359−6366] prompt us to question the reliability of predicting the $\Delta C_p°$ values of the enzyme−ligand complexes from their X-ray crystallographic data. Arguments are presented that certain intrinisic limitations of the crystallographic data preclude kinetic and thermodynamic predictions about the enzyme−ligand complexes and enzyme catalysis.

Following our initial demonstration that the 3′,5′-ADP fragment of coenzyme A of a chromogenic substrate, indolepropionyl-CoA (IPCoA[1]), played a crucial role in the pig kidney medium-chain acyl-CoA dehydrogenase (MCAD)-catalyzed reaction (*1*), we became interested in the role of distal fragments of the coenzyme A moiety during enzyme catalysis. On the basis of the X-ray crystallographic data of the pig liver MCAD−$C_8$-CoA complex (*2*), it has been known that the 3′-phosphate group constitutes the distal-most fragment of the coenzyme A structure (about 15 Å removed from the enzyme active site), and is fully exposed to the exterior solvent environment. One of the oxygen atoms (viz., O8A2) of the 3′-phosphate residue is located 3.33 Å from the side chain hydroxyl oxygen (OG) of Ser191, suggesting the formation of a potential hydrogen bond between the above moieties (Figure 1). The crystallographic data also suggested the presence of a water molecule (HOH-986) in the vicinity of the 3′-phosphate (not shown in Figure 1), which had the potential to form hydrogen bonds with all the phosphate oxygens, viz., O7A2, O8A2, and O9A2 of the coenzyme A moiety.

A comparison between the amino acid sequence of pig liver (A. W. Strauss, personal communication) and human liver MCADs (*3*) reveals that Ser191 in the pig liver enzyme is substituted by Asn191 in the human liver enzyme.

† This work was supported by grants from the National Science Foundation (MCB-9507292) and the American Heart Association, National Center (AHA-96008200).

* To whom correspondence should be addressed.

[1] Abbreviations: MCAD, medium-chain acyl-CoA dehydrogenase; FAD, flavin adenine dinucleotide; OcaCoA, octanoyl-CoA; OceCoA, 2-octenoyl-CoA; IPCoA, 3-indolepropionyl-CoA; IACoA, *trans*-3-indoleacryloyl-CoA; $FcPF_6$, ferricenium hexafluorophosphate; $\Delta G°$, standard free energy change; $\Delta H°$, standard enthalpy change; $\Delta S°$, standard entropy change; $K_a$, association constant; $\Delta C_p°$, standard heat capacity change.

S0006-2960(98)00949-0 CCC: $15.00 
Published on Web 08/20/1998

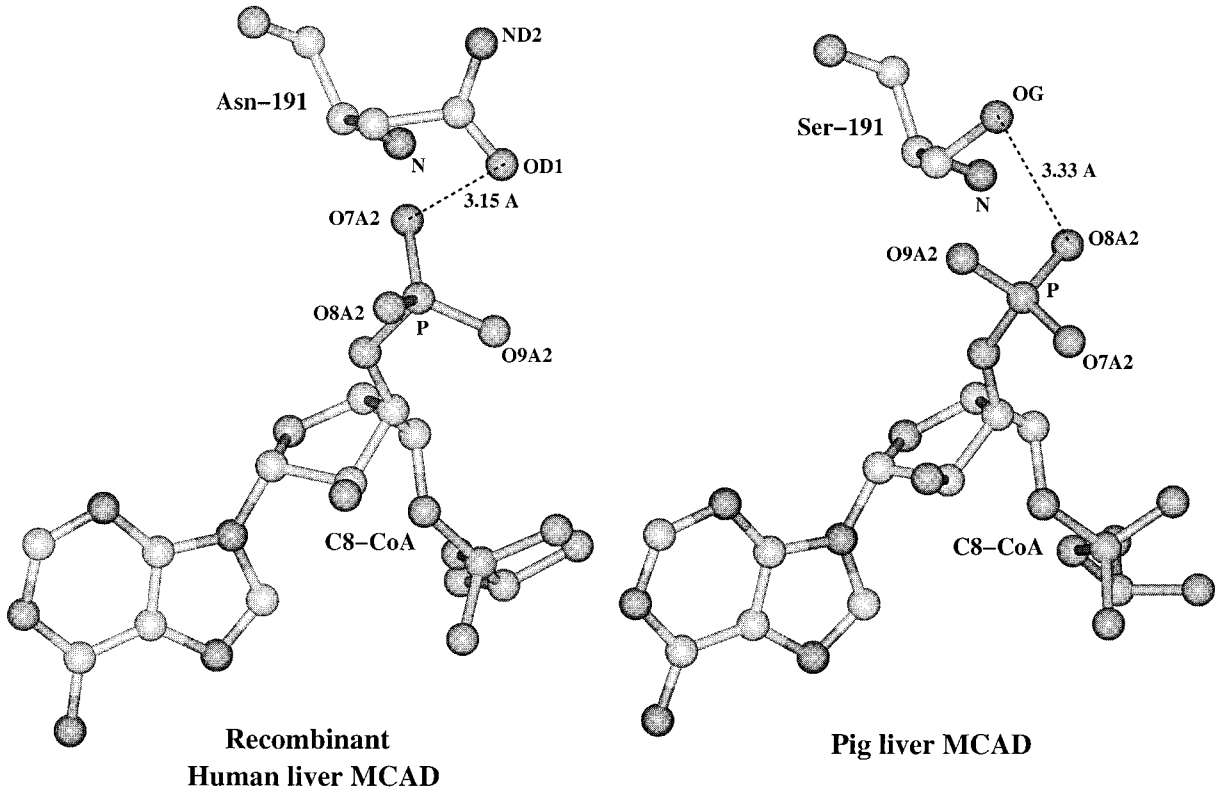


FIGURE 1: Spatial relationships between the 3′-phosphate group of $C_8$-CoA and the side chain of amino acid residue 191. Whereas residue 191 is contributed by Ser in the case of pig liver MCAD (right), it is contributed by Asn in the case of human liver MCAD (left). For clarity, only the part of the $C_8$-CoA structure in the vicinity of residue 191 has been shown. The atom labels are as denoted in the corresponding PDB files. The hydrogen bonding between corresponding atoms of the 3′-phosphate group and the side chains of Ser191 (right) and Asn191 (left) is shown.

However, given a marked structural similarity between the pig liver and a double mutant (Thr262 → Glu/Glu376 → Gly) human liver enzyme (*4*), Asn191 of the human liver enzyme occupies more or less the same position as Ser191 of the pig liver enzyme (Figure 1). The $C_8$-CoA residue of the human liver enzyme, however, exhibits a 1.2 Å rmsd from the corresponding residue bound to the pig liver enzyme. The 3′-phosphate group of $C_8$-CoA (bound to the human liver enzyme) is rotated by 16° compared to that bound to the pig liver enzyme. Such a spatial feature allows for the juxtaposition of the amide oxygen (OD1) of the side chain group of Asn191 to another oxygen (O7A2) atom of the 3′-phosphate group of $C_8$-CoA (see Figure 1). The distance between the above residues can be determined to be 3.15 Å, once again suggesting a potential hydrogen bond between the above residues.

We recently elaborated on the detailed microscopic pathways for the octanoyl-CoA-dependent reaction of both pig kidney (*5*, *6*) and recombinant human liver (*7*) enzymes. For both these enzymes, the rate-limiting step was deduced to be the dissociation "off-rate" of the reaction product, octenoyl-CoA, from the oxidized enzyme site (*8*, *9*). This observation was in marked contrast to the butyryl-CoA- and IPCoA-dependent reactions, as with the latter substrates, the rate-limiting step of the enzyme was the forward rate constant of the reductive half-reaction (*10*−*12*).

Given these mechanistic precedents, we investigated the effects of deletion of the 3′-phosphate group from both octanoyl-CoA and butyryl-CoA as enzyme substrates (*8*). The steady-state kinetic data revealed that whereas the deletion of the 3′-phosphate group impaired the turnover rate of the butyryl-CoA-dependent reaction by 4-fold, it enhanced the turnover rate of the octanoyl-CoA-dependent reaction by 4-fold. These results somewhat contradict the initial report of Frerman et al. (*51*), as well as the conclusions derived on the basis of the X-ray crystallographic data (*2*). However, to probe the molecular basis of the above effects, we investigated the transient kinetics for the reductive half-reaction, oxidative half-reaction, and the dissociation off-rate constants of the reaction products from the oxidized enzyme site (*8*). It was observed that although the deletion of the 3′-phosphate group from both octanoyl-CoA and butyryl-CoA substrates had less pronounced and nonspecific effects on the oxidative half-reaction of the enzyme, it impaired the reductive half-reaction of the enzyme by 2−10-fold, and it enhanced the dissociation off-rates of the enoyl-CoA products from the oxidized enzyme site by 2−13-fold, respectively (*8*). Since the latter step served as the rate-limiting step during the octanoyl-CoA-dependent reaction (*9*), the steady-state turnover rate of the enzyme was found to be increased. Such an advantage was not realized in the case of butyryl-CoA-dependent reaction, since with this substrate, the rate-limiting step was conformed by the flavin reduction step, and the impairment of the latter step (upon deletion of the 3′-phosphate group from butyryl-CoA) resulted in a decrease in the turnover rate of the enzyme (*8*).

We recently became interested in investigating the thermodynamic aspects of the enzyme−ligand interactions via isothermal microcalorimetry (*13*, *14*). This technique allows for the direct determination of the enthalpic changes ($\Delta H°$) and the association constant ($K_a$) of the enzyme−ligand

complex from a single titration experiment, and given this information, the standard free energy ($\Delta G°$) and entropic changes ($\Delta S°$) of the enzyme-ligand interactions are easily deduced. With pig kidney MCAD, the above approach led to the revelation that whereas the binding of octenoyl-CoA to the enzyme (at 25 °C) was predominantly enthalpically driven ($\Delta G° = -8.8$ kcal/mol, $\Delta H° = -10.3$ kcal/mol, and $T\Delta S° = -1.5$ kcal/mol), the binding of our thoroughly studied chromophoric reaction product (*15*−*18*), indoleacryloyl-CoA (IACoA), was favored by both enthalpic and entropic contributions ($\Delta G° = -7.4$ kcal/mol, $\Delta H° = -3.7$ kcal/mol, and $T\Delta S° = 3.7$ kcal/mol; *14*). The heat capacity changes ($\Delta C_p°$) for the binding of the above ligands were discerned to be $-0.37$ and $-0.24$ kcal mol$^{-1}$ K$^{-1}$, respectively (*13*, *14*). Given these, we sought to discern the specific thermodynamic contributions of the 3′-phosphate group of octanoyl-CoA in stabilizing the ground- and transition-state structures formed during enzyme catalysis. To dissect whether such contributions were partly or fully given by the potential hydrogen bonds between OD1 of Asn191 and O7A2 of $C_8$-CoA (see Figure 1), we performed these studies utilizing both wild-type and Asn191 → Ala site-directed mutant enzymes, as well as normal (i.e., phosphorylated) and 3′-dephosphorylated forms of octanoyl-CoA and octenoyl-CoA. Since the X-ray crystallographic structures of both pig liver and human liver enzymes in the absence and presence of $C_8$-CoA are known (*2*, *4*), we hoped to elucidate the relationships between the experimentally determined $\Delta C_p°$ values (for the binding of normal and 3′-dephosphorylated $C_8$-CoAs) and the changes in the solvent-accessible polar and nonpolar surface areas upon enzyme−ligand interactions.

## MATERIALS AND METHODS

*Materials.* Octanoyl-CoA, CoA (sodium salt), and EDTA were purchased from Sigma. Octenoic acid was purchased from Pfaltz and Bauer. All other reagents were of analytical grade.

*Method.* The site-specific mutation of Asn191 to Ala (N191A) in human liver medium-chain acyl-CoA dehydrogenase (MCAD) was created in the laboratory of A. W. Strauss (Washington University, St. Louis, MO) and was obtained as a gift. The N191A mutant sequence was restriction-digested out of pBluescript II (KS−) with *Xba*I and *Hin*dIII, purified by agarose gel electrophoresis, ligated at *Xba*I−*Hin*dIII sites in the expression plasmid pTrc 99B using T4 DNA ligase, and transformed into the DH5α cells and propagated essentially as described by Peterson et al. (*19*). The wild-type and N191A mutant enzymes were expressed in the *Escherichia coli* TG1 cells and purified according to Peterson et al. (*19*).

All experiments were performed in 50 mM potassium phosphate (pH 7.6) containing 10% glycerol and adjusted to an ionic strength of 175 mM by addition of 3 M KCl. The enzymes were assayed by monitoring the reduction of ferricenium hexafluorophosphate ($FcPF_6$) at 300 nm ($\epsilon_{300} = 4.3$ mM$^{-1}$ cm$^{-1}$; *20*) in a reaction mixture containing 100 $\mu$M octanoyl-CoA and 350 $\mu$M $FcPF_6$ as described previously (*5*−*7*). Since the UV−vis normalized spectra of the wild-type and mutant enzymes were nearly identical, their concentrations were determined using an extinction coefficient of 15.4 mM$^{-1}$ cm$^{-1}$ at 446 nm (*21*).

The CoA derivative 2-octenoyl-CoA was synthesized by the mixed anhydride procedure of Bernert and Sprecher (*22*) as described previously (*5*−*8*). The 3′-dephosphorylated form of octenoyl-CoA was prepared as described by Peterson and Srivastava (*8*). The concentrations of 2-octenoyl-CoA and 3′-dephosphooctenoyl-CoA were determined using an extinction coefficient of 20.4 mM$^{-1}$ cm$^{-1}$, while the octanoyl-CoA and 3′-dephosphooctanoyl-CoA concentrations were determined using an extinction coefficient of 15.6 mM$^{-1}$ cm$^{-1}$ (*8*).

*Steady-State and Transient Kinetic Experiments.* The steady-state kinetic experiments for the enzyme-catalyzed reactions were performed on a Perkin-Elmer Lambda 3B spectrophotometer with a 1 cm path length cuvette (*1*, *5*−*8*). The single-wavelength transient kinetic experiments were performed on an Applied Photophysics SX-17 MV stopped-flow system (optical path length of 10 mm, dead time of 1.3−1.5 ms; *5*−*8*, *10*, *11*). The stopped-flow system was configured in a single mixing mode. In this mode, the contents of syringes A and B were diluted by 50%. The stopped-flow kinetic traces were analyzed by the data analysis package provided by Applied Photophysics.

The reductive half-reaction rate constants for the octanoyl-CoA- and 3′-dephosphooctanoyl-CoA-dependent reactions with the wild-type and mutant enzymes were determined by mixing the above species via the stopped-flow syringes (under the pseudo-first-order conditions where [E-FAD] ≪ [substrate]) and monitoring the time-dependent absorption changes at 450 nm (*5*−*10*). The temperature-dependent transient kinetic studies were performed as described by Qin and Srivastava (*14*).

*Isothermal Titration Microcalorimetry.* The isothermal calorimetric experiments were performed on a MCS isothermal titration microcalorimeter (ITC) from Microcal Inc., as described by Srivastava et al. (*13*). The sample cell was filled with 1.8 mL of the buffer (control) or enzyme solution (effective volume of 1.36 mL). The injector was filled with 250 $\mu$L of the ligand. The titration was initiated by the first (preliminary) injection of 1 $\mu$L, followed by 59 injections (4 $\mu$L each) of the ligand. During the experiment, the enzyme solution was stirred at a constant rate of 400 rpm. The enzyme concentration was adjusted by 2% to allow for dilution following a buffer rinse of the cell (*13*).

All of the calorimetric data were presented after correction for the background. Since the titration produced a small turbidity in the enzyme solution, the background heat was somewhat larger than that obtained for the dilution of the ligand in the buffer medium, and the heat produced at the end of the titration (where the enzyme was saturated by the ligand) was taken as the measure of the background heat. The experimental data were analyzed according to Wiseman et al. (*23*).

The data analysis produced three parameters, viz., stoichiometry ($n$), association constant ($K_a$), and the standard enthalpy changes ($\Delta H°$) for the binding of the ligand to MCAD. The standard free energy change ($\Delta G°$) for the binding was calculated according to the relationship $\Delta G° = -RT \ln K_a$. Given the magnitudes of $\Delta G°$ and $\Delta H°$, the standard entropy changes ($\Delta S°$) for the binding process were calculated according to the standard thermodynamic equation $\Delta G° = \Delta H° - T\Delta S°$.

*Determination of Solvent-Accessible Nonpolar and Polar Surface Areas.* The solvent-accessible nonpolar and polar surface areas of both pig liver and recombinant human liver MCADs, and of $C_8$-CoA and 3′-dephospho-$C_8$-CoA, were determined (for heavy atoms) according to the algorithm of Lee and Richards (*24*), using a probe with a radius of 1.4 Å, via the ProState module of Homology-97 (Molecular Simulations Inc.). The coordinates of pig liver MCAD in the absence (3MDD) and presence of $C_8$-CoA (3MDE) and double mutants (Thr255 → Glu/Glu376 → Gly) of human liver MCAD in the absence (1EGD) and presence (1EGC) of $C_8$-CoA were obtained from the Brookhaven Protein Data Bank. To simplify the calculation, we separated a single subunit from each of the tetrameric proteins, and interfaced with a 4 Å perimeter of crystallographic water molecules, with the aid of Insight-II(97) software (Molecular Simulations Inc.).

With $C_8$-CoA-bound enzymes, the water-accessible surface area calculations were performed with bound $C_8$-CoA, and after removal of $C_8$-CoA from the enzyme site. Prior to calculation, free $C_8$-CoA (i.e., after separation from the enzyme site) was subjected to energy minimization with the aid of Discover-97 (Molecular Simulations Inc.) as recently described by Srivastava and Peterson (*25*). The latter stratagem was to release any constraint imposed by the protein structure within its resident site. The 3′-dephosphorylated form of $C_8$-CoA was created by deleting the terminal 3′-phosphate group from the enzyme-bound $C_8$-CoA structure.

The water-accessible total surface area (Connolly surface) in the vicinity of the enzyme-bound $C_8$-CoA was calculated by Insight-II(97), using a probe radius of 1.4 Å (*42*).

## RESULTS

*Isothermal Microcalorimetric Studies for the Binding of Ligands to Human Liver MCAD.* Figure 2 shows the isothermal microcalorimetric data for the titration of wild-type human liver medium-chain acyl-CoA dehydrogenase (MCAD) with octenoyl-CoA in the standard phosphate buffer at 25 °C. The top panel shows the raw calorimetric data. The emergence of negative peaks following each injection was indicative of the fact that the binding of octenoyl-CoA to the enzyme produced heat (an exothermic process). The magnitude of heat produced per injection was determined by integration of the area under the individual peak. Note that as the titration progressed, the area under the peak progressively became smaller, due to increased occupancy of the enzyme site by octenoyl-CoA. The bottom panel of Figure 2 shows the plot of the amount of heat generated per injection as a function of the molar ratio of octenoyl-CoA to the enzyme. The solid smooth line is the best fit of the experimental data according to Wiseman et al. (*23*), for the values for stoichiometry ($n$), the association constant ($K_a$), and the standard enthalpic changes ($\Delta H°$) of the MCAD−octenoyl-CoA complex of 0.93 ± 0.01, (9.8 ± 0.6) × $10^5$ $M^{-1}$, and −18.3 ± 0.3 kcal/mol, respectively. The $K_a$ value is translated into the standard free energy changes ($\Delta G° = -RT \ln K_a$) of −8.2 kcal/mol, taking into account the standard state being equal to 1 M. From these data, the standard entropic changes ($\Delta S°$) for the above binding process could be discerned ($\Delta S° = -\Delta G°/T + \Delta H°/T$) to be −33.8 cal $mol^{-1}$ $K^{-1}$.

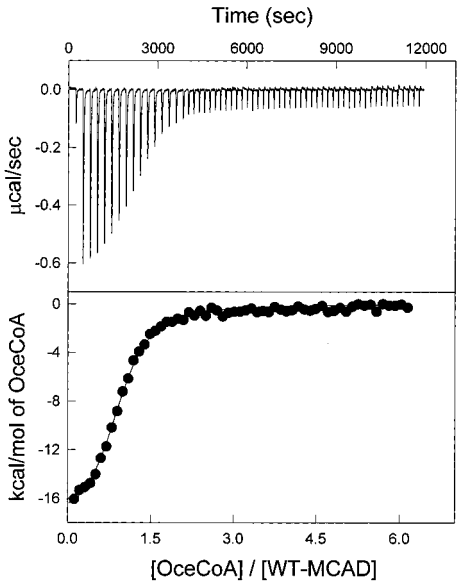


FIGURE 2: Isothermal microcalorimetric titration data for the interaction of octenoyl-CoA with wild-type human liver MCAD. A 1.8 mL solution of the enzyme (10 $\mu$M) was titrated with 60 aliquots of 4 $\mu$L each (except for the first aliquot which was 1 $\mu$L) of a 300 $\mu$M stock solution of octenoyl-CoA in the standard phosphate buffer at 25 °C. The upper panel shows the raw calorimetric data, and the bottom panel shows the relationship between the amount of heat produced per mole of ligand and the molar ratio of the ligand to the enzyme. The solid smooth lines are the best fit of the experimental data according to Wiseman et al. for a stoichiometry ($n$) of 0.93 ± 0.01, an association constant for the enzyme−ligand complex ($K_a$) of (9.8 ± 0.6) × $10^5$ $M^{-1}$, and the standard enthalpic changes ($\Delta H°$) of −18.3 ± 0.3 kcal/mol.

To our surprise, the average $\Delta H°$ value (see below) obtained for the binding of octenoyl-CoA to human liver MCAD was found to be 6.8 kcal/mol more favorable (i.e., negative) than that for the binding of octenoyl-CoA to the pig kidney enzyme (*13*). In contrast, the $\Delta G°$ value for the above process was only 0.5 kcal/mol less favorable in the case of the human liver enzyme than in the case of the pig kidney enzyme (*13*). Hence, the binding of octenoyl-CoA to the human liver enzyme was 7.3 kcal/mol entropically less favorable than that to the pig kidney enzyme.

To ascertain the influence of the 3′-phosphate group of octenoyl-CoA on the energetics of binding to human liver MCAD, we performed the above isothermal microcalorimetric titration experiment involving 3′-dephosphooctenoyl-CoA (Figure 3A). The analysis of the experimental data (as described above) yielded the following values of $n$, $K_a$, and $\Delta H°$: 1.0 ± 0.01, (7.6 ± 0.2) × $10^4$ $M^{-1}$, and −16.5 ± 0.2 kcal/mol, respectively. From these values, $\Delta G°$ and $\Delta S°$ were determined to be −6.7 kcal/mol and −33 cal $mol^{-1}$ $K^{-1}$, respectively. Upon comparison of the data of Figures 2 and 3A, it is apparent that the deletion of the 3′-phosphate group results in (unfavorable) increases in both $\Delta G°$ and $\Delta H°$ values of 1.5 and 1.8 kcal/mol, respectively. Consistently, the deletion of the 3′-phosphate group from octenoyl-CoA favorably increases the $T\Delta S°$ value (at 25 °C) by 0.3 kcal/mol. An average of three independent titrations of wild-type human liver MCAD by octenoyl-CoA and 3′-dephosphooctenoyl-CoA yielded values for the free energy ($\Delta\Delta G°$) and enthalpic ($\Delta\Delta H°$) contribution of the 3′-phosphate group of 1.2 and 2.0 kcal/mol, respectively.

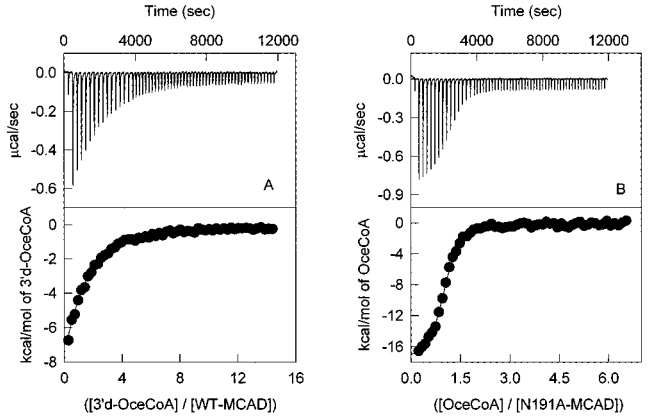


FIGURE 3: Isothermal microcalorimetric titration data for the interactions of 3′-dephosphooctenoyl-CoA with wild-type human liver MCAD (left panel, A) and octenoyl-CoA with N191A mutant human liver MCAD (right panel, B). The experimental conditions were the same as in Figure 1. The upper and lower panels represent the raw calorimetric and fitted data, respectively. In panel A, the concentrations of the wild-type enzyme and the 3′-dephospho-octenoyl-CoA were 10 and 800 $\mu$M, respectively. The solid smooth line is the best fit of the experimental data for $n = 1.0 \pm 0.01$, $K_a = (7.6 \pm 0.2) \times 10^4$ M$^{-1}$, and $\Delta H° = -16.5 \pm 0.2$ kcal/mol. In panel B, the concentrations of the N191A mutant enzyme and octenoyl-CoA were 10 and 300 $\mu$M, respectively. The solid smooth line is the best fit of the experimental data for $n = 1.0 \pm 0.01$, $K_a = (2.1 \pm 0.1) \times 10^6$ M$^{-1}$, and $\Delta H° = -18.0 \pm 0.3$ kcal/mol.

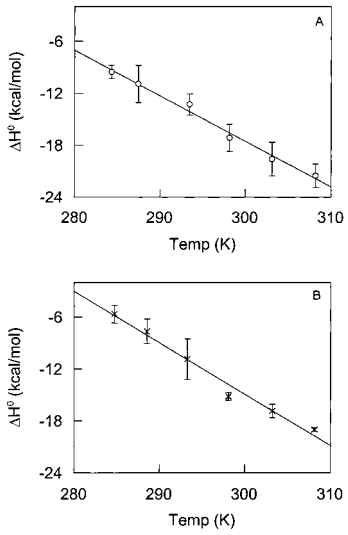


FIGURE 4: Temperature dependence of $\Delta H°$ on the interaction of octenoyl-CoA (A) and 3′-dephosphooctenoyl-CoA (B) with wild-type human liver MCAD. In panel A, the solid line is the linear regression analysis of the experimental data for a slope ($\Delta C_p°$ ) of $-0.53 \pm 0.03$ kcal mol$^{-1}$ K$^{-1}$ and an intercept (at 0 K) of $140 \pm 9$ kcal/mol. In panel B, the solid line is the linear regression analysis of the experimental data for a slope ($\Delta C_p°$) of $-0.59 \pm 0.04$ kcal mol$^{-1}$ K$^{-1}$ and an intercept (at 0 K) of $163 \pm 12$ kcal/mol.

To what extent are the total enthalpic and free energy contributions of the 3′-phosphate group given by the hydrogen bonding between OD1 of the side chain residue of Asn191 and O7A2 of the 3′-phosphate group of $C_8$-CoA (see Figure 1)? To probe this, we performed the above microcalorimetric titration for the binding of octenoyl-CoA to Asn191 → Ala (N191A) mutant human liver MCAD at 25 °C. The data are shown in Figure 3B. The analysis of the binding isotherm (as described above) for the titration results of Figure 3B yielded the following values of $n$, $K_a$, and $\Delta H°$: $1.0 \pm 0.01$, $(2.1 \pm 0.1) \times 10^6$ M$^{-1}$, and $-18.0 \pm 0.3$ kcal/mol, respectively. An average of three independent titrations yielded the following values of $\Delta G°$, $\Delta H°$, and $T\Delta S°$: $-8.6 \pm 0.03$, $-17.7 \pm 0.05$, and $-9.0 \pm 0.4$ kcal/mol, respectively. Note that the latter parameters are similar to those obtained for the binding of octenoyl-CoA to the wild-type enzyme (see above). A cumulative account of the experimental data of Figures 2 and 3 reveals that the enthalpic contribution of the 3′-phosphate group of octenoyl-CoA is derived from the London−van der Waals interactions, and not from the hydrogen bonding between OD1 of Asn191 and O7A2 of $C_8$-CoA (see Figure 1 and the Discussion).

*Temperature Dependence of the Thermodynamic Parameters.* To account for the effect of deletion of the 3′-phosphate group of octenoyl-CoA on the heat capacity changes ($\Delta C_p°$), upon formation of the corresponding enzyme−ligand complexes, we investigated the temperature dependence of $\Delta H°$ for the binding of both octenoyl-CoA and 3′-dephosphooctenoyl-CoA to the wild-type human liver MCAD. Figure 4A shows that as the temperature increases, $\Delta H°$ linearly decreases (i.e., becomes more favorable). The solid line is the linear regression analysis of the experimental data for the slope and intercept of $-0.53 \pm 0.03$ kcal mol$^{-1}$ K$^{-1}$ and $140 \pm 9$ kcal/mol, respectively. Of these, the slope serves as a measure of $\Delta C_p°$ for the binding of octenoyl-CoA to the enzyme. It should be noted that the latter value is far more negative than that determined for the binding of octenoyl-CoA to pig kidney MCAD ($\Delta C_p° = -0.37$ kcal mol$^{-1}$ K$^{-1}$; *13*).

Figure 4B shows the temperature dependence of $\Delta H°$ for the binding of 3′-dephosphooctenoyl-CoA to the wild-type human liver MCAD. The linear regression analysis of the experimental data yields a $\Delta C_p°$ value of $-0.59 \pm 0.04$ kcal mol$^{-1}$ K$^{-1}$. Note that the latter value is about 11% higher than that obtained for the binding of octenoyl-CoA to human liver MCAD (Figure 4A). Such a difference is qualitatively consistent with the fact that the deletion of the 3′-phosphate from octenoyl-CoA increases the relative hydrophobicity of the ligand, and thus, in turn, increases the magnitude of $\Delta C_p°$.

Table 1 summarizes the temperature dependence of all the thermodynamic parameters for the binding of octenoyl-CoA and 3′-dephosphooctenoyl-CoA to human liver MCAD. It should be pointed out that all the microcalorimetric titration experiments reported in Table 1 have been performed (at least) in triplicate, and the values are the average of these independent experiments. From the data of Table 1, it is evident that as the temperature increases, whereas $\Delta G°$ values for the binding of both octenoyl-CoA and 3′-dephospho-octenoyl-CoA to the enzyme remain more or less constant, the corresponding $\Delta H°$ and $T\Delta S°$ parameters decrease, resulting in a large enthalpy−entropy compensation effect. Panels A and B of Figure 5 show the plots of $\Delta G°$ and $\Delta H°$ for the individual ligands as a function of $T\Delta S°$. Note that when $T\Delta S°$ attains a value of zero, $\Delta G°$ becomes equal to $\Delta H°$. The temperature at which the above relationship is attained can be calculated from the plots of panels A and B of Figure 4. Such temperatures for the binding of octenoyl-CoA and 3′-dephosphooctenoyl-CoA to human liver MCAD were discerned to be 7.2 and 15.5 °C, respectively. It should be pointed out that the above temperatures are 16.6 and 8.3 °C lower than that obtained for the binding of octenoyl-CoA

Table 1: Summary of the Isothermal Microcalorimetric Titration Results[a]

| ligand | temp (K) | no. of expts | $n$ | $K_a$ ($\times 10^6$ $M^{-1}$) | $\Delta H°$ (kcal/mol) | $\Delta G°$ (kcal/mol) | $T\Delta S°$ (kcal/mol) |
|---|---|---|---|---|---|---|---|
| OceCoA | 284.3 | 3 | $0.89 \pm 0.03$ | $2.6 \pm 0.9$ | $-9.5 \pm 0.8$ | $-8.3 \pm 0.2$ | $-1.2 \pm 0.9$ |
| | 287.5 | 3 | $0.93 \pm 0.06$ | $2.6 \pm 1.0$ | $-10.9 \pm 2.1$ | $-8.4 \pm 0.3$ | $-2.6 \pm 2.4$ |
| | 293.5 | 3 | $1.0 \pm 0.02$ | $1.3 \pm 0.7$ | $-13.3 \pm 1.2$ | $-8.2 \pm 0.3$ | $-5.1 \pm 1.3$ |
| | 298.2 | 3 | $0.98 \pm 0.06$ | $1.3 \pm 0.5$ | $-17.2 \pm 1.6$ | $-8.3 \pm 0.2$ | $-8.9 \pm 1.8$ |
| | 303.1 | 5 | $1.0 \pm 0.1$ | $1.6 \pm 0.9$ | $-19.6 \pm 1.9$ | $-8.5 \pm 0.4$ | $-11.1 \pm 2.2$ |
| | 308.2 | 4 | $1.2 \pm 0.06$ | $0.8 \pm 0.4$ | $-21.5 \pm 1.3$ | $-8.2 \pm 0.3$ | $-13.3 \pm 1.6$ |
| dOceCoA | 284.5 | 4 | $0.95 \pm 0.07$ | $0.25 \pm 0.07$ | $-5.7 \pm 1.0$ | $-7.0 \pm 0.2$ | $1.3 \pm 1.2$ |
| | 288.6 | 3 | $1.0 \pm 0.1$ | $0.19 \pm 0.06$ | $-8.8 \pm 2.2$ | $-7.0 \pm 0.2$ | $-1.8 \pm 2.3$ |
| | 293.3 | 3 | $0.98 \pm 0.1$ | $0.11 \pm 0.03$ | $-12.3 \pm 3.0$ | $-6.8 \pm 0.1$ | $-5.6 \pm 3.2$ |
| | 298.1 | 3 | $1.0 \pm 0.1$ | $0.32 \pm 0.4$ | $-15.2 \pm 0.4$ | $-7.1 \pm 0.8$ | $-8.0 \pm 0.4$ |
| | 303.2 | 3 | $1.0 \pm 0.05$ | $0.073 \pm 0.006$ | $-16.9 \pm 0.8$ | $-6.7 \pm 0.06$ | $-10.1 \pm 0.8$ |
| | 308.1 | 3 | $1.1 \pm 0.1$ | $0.050 \pm 0.004$ | $-19.2 \pm 0.5$ | $-6.6 \pm 0.05$ | $-12.6 \pm 0.5$ |

[a] OceCoA and d-OceCoA represent octenoyl-CoA and 3′-dephosphooctenoyl-CoA, respectively.

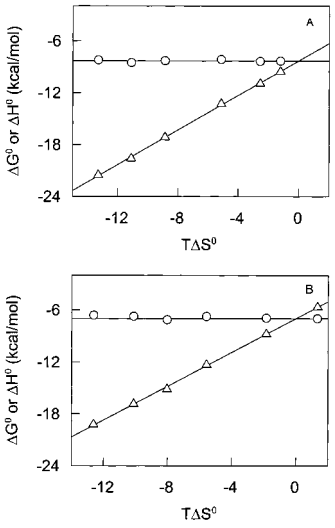


FIGURE 5: Enthalpy−entropy compensation plots for the binding of octenoyl-CoA (A) or 3′-dephosphooctenoyl-CoA (B) to the wild-type human liver enzyme. In panels A and B, the experimental data for $\Delta G°$ and $\Delta H°$ are represented by open circles and open triangles, respectively. The linear regression analysis for the data of panel A of $\Delta H°$ vs $T\Delta S°$ yields magnitudes for the slope and intercept of $1.0 \pm 0.01$ and $-8.3 \pm 0.1$ kcal/mol, respectively. In panel B, such an analysis yields magnitudes for the slope and intercept of $0.98 \pm 0.02$ and $-7.0 \pm 0.1$ kcal/mol, respectively.

to the pig kidney enzyme (*13*). At this time, we do not understand the molecular basis of these effects.

*Effect of the Asn191 → Ala Mutation on the Steady-State and Transient Kinetics of the Reductive Half-Reaction.* We previously reported the effect of deletion of the 3′-phosphate group from octanoyl-CoA on the steady-state kinetics and the reductive half-reaction of wild-type human liver MCAD (*8*). To ascertain whether the potential hydrogen bonding between OD1 of Asn191 and O7A2 of $C_8$-CoA (see Figure 1) exhibits any influence on the transition state(s) of the enzyme catalysis, we undertook a comparative steady-state kinetic investigation of the wild-type and N191A mutant human liver MCAD-catalyzed reactions. Table 2 summarizes the steady-state kinetic parameters of these enzymes utilizing octanoyl-CoA as a substrate and ferricenium hexafluorophosphate ($FcPF_6$) as an electron acceptor. Note that the above mutation had practically no influence on either apparent $K_m$ values of octanoyl-CoA and $FcPF_6$ or the $k_{cat}$ of the enzyme.

However, given that the rate-limiting step of the octanoyl-CoA-dependent reaction is the dissociation off-rate of the

Table 2: Steady-State Kinetic Parameters for the Wild-Type and Asn191 → Ala (N191A) Mutant of Human Liver Medium-Chain Acyl-CoA Dehydrogenase[a]

| variable substrate | fixed substrate | $K_m$ ($\mu$M) | $k_{cat}$ ($s^{-1}$) |
|---|---|---|---|
| wild-type | | | |
| OcaCoA[b] | $FcPF_6$ (350 $\mu$M) | $2.1 \pm 0.6$ | $12.1 \pm 0.6$ |
| $FcPF_6$ | OcaCoA (50 $\mu$M) | $69 \pm 5$ | $16.4 \pm 0.4$ |
| N191 mutant | | | |
| OcaCoA | $FcPF_6$ (350 $\mu$M) | $1.6 \pm 0.2$ | $11.2 \pm 0.3$ |
| $FcPF_6$ | OcaCoA (50 $\mu$M) | $85 \pm 14$ | $15.2 \pm 0.7$ |

[a] OcaCoA and $FcPF_6$ represent octanoyl-CoA and ferricenium hexafluorophosphate, respectively. [b] The steady-state kinetic parameters for the octanoyl-CoA-dependent reaction of the wild-type enzyme, recently determined, are slightly different from those reported previously ($K_m^{octanoyl-CoA} = 2.6 \pm 0.4$ and $k_{cat} = 15.6 \pm 0.5$ $s^{-1}$; *8*).

reaction product, octenoyl-CoA (*8*, *9*), the lack of influence of the Asn191 → Ala mutation on the turnover rate of the enzyme may not provide any information about whether the potential hydrogen bond (between OD1 of Asn191 and O7A2 of $C_8$-CoA) stabilizes the transition state, formed during the chemical transformation (i.e., the flavin reduction) step. The latter consideration has been important particularly from the point of view that the improvement of the chemical transformation step has been the dominating feature of the natural selection process (*32*, *33*). To probe this, we investigated the effect of the Asn191 → Ala mutation on the reductive half-reaction of the enzyme, utilizing octanoyl-CoA as a substrate. Figure 6 shows the stopped-flow traces (at 450 nm) upon mixing of either 20 $\mu$M wild-type or 20 $\mu$M N191A mutant enzyme with 200 $\mu$M octanoyl-CoA. The experimental data are best fitted for the biphasic rate equations with fast and slow relaxation rate constants of $476 \pm 6$ and $39 \pm 1$ $s^{-1}$ in the case of the wild-type enzyme, and $466 \pm 3$ and $56 \pm 1$ $s^{-1}$ in the case of the N191A mutant enzyme, respectively. These data clearly attest to the fact that the Asn191 → Ala mutation does not alter the rate of the reductive half-reaction of the enzyme. Hence, neither the reductive half-reaction nor the steady-state kinetic parameters of the enzyme are affected upon Asn191 → Ala mutation. Clearly, there is no functional role of the putative hydrogen bonding (between OD1 of Asn191 and O7A2 of $C_8$-CoA) in stabilizing either the ground- or transition-state structure during the enzyme−ligand interaction and enzyme catalysis.

*Effect of Deletion of the 3′-Phosphate Group from Octanoyl-CoA on the Energy of Activation ($E_a$) during the*

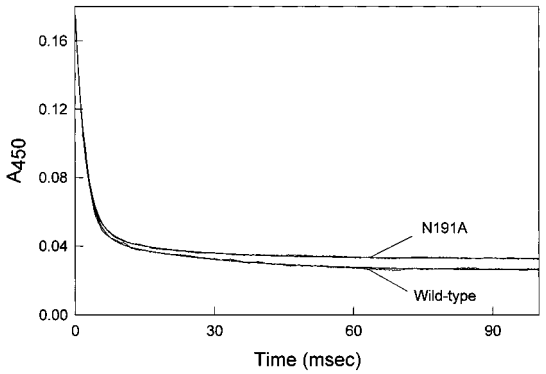


FIGURE 6: Transient kinetics for the octanoyl-CoA-dependent reductive half-reaction of wild-type and N191A mutant human liver MCADs. The stopped-flow traces show the decrease in absorption (at 450 nm) due to the reduction of the enzyme-bound FAD by octanoyl-CoA at 5 °C. The after-mixing concentrations of wild-type and N191A enzymes and octanoyl-CoA were 10, 10, and 100 $\mu$M, respectively. The solid smooth lines are the best fits of the experimental data to the double-exponential rate equation. The fast ($k_{fast}$) and slow ($k_{slow}$) relaxation rate constants and their corresponding amplitudes, $\Delta A_{fast}$ and $\Delta A_{slow}$, for the reaction of octanoyl-CoA with the wild-type enzyme were 476 ± 6, 39.0 ± 0.9, 0.13 ± 0.001, and 0.021 ± 0.003, respectively. The corresponding parameters for the reaction of octanoyl-CoA with N191A mutant enzyme were found to be 466 ± 3.1, 55.5 ± 0.9, 0.134 ± 0.0007, and 0.016 ± 0.0002, respectively.

*Reductive Half-Reaction of the Wild-Type Enzyme.* The free energy ($\Delta\Delta G°$) and enthalpic ($\Delta\Delta H°$) contributions of the 3′-phosphate group of octenoyl-CoA, derived from the microcalorimetric titration data (Figures 2 and 3A), can be (qualitatively) taken as a measure of the effect of the 3′-phosphate group in stabilizing the ground state of the enzyme−substrate complex. It does not provide any information about the role of the 3′-phosphate group in stabilizing the transition state of the octanoyl-CoA-dependent reductive half-reaction (i.e., the "chemistry" of flavin reduction) of the enzyme. To ascertain the latter, we investigated the temperature dependence of the octanoyl-CoA- and 3′-dephosphooctanoyl-CoA-dependent reductive half-reactions of the enzyme.

We previously demonstrated that both the octanoyl-CoA- and 3′-dephosphooctanoyl-CoA-dependent reactions conformed to the biphasic kinetics (*8*), of which the fast rate constant was decreased by about 2-fold upon deletion of the 3′-phosphate group from octanoyl-CoA (*8*). The slow phase was found to remain unaffected or, at the best, slightly increased under the above condition. The transient kinetics for the reduction of the enzyme-bound FAD by octanoyl-CoA and 3′-dephosphooctanoyl-CoA were ascertained by mixing the above reactants under pseudo-first-order conditions ([MCAD−FAD] ≪ [ligand]) via the stopped-flow syringes, followed by recording the time-dependent absorption changes at 450 nm. Under the above conditions, both fast and slow rate constants showed a (apparent) hyperbolic dependence on substrate concentrations beyond 100 $\mu$M, suggesting higher binding affinities ($K_d \leq 25$ $\mu$M) of these substrates within their corresponding Michaelis complexes.

We performed the stopped-flow kinetic experiments at increasing temperatures, and the resultant reaction traces were analyzed by the biphasic rate equation as described previously (*5*−*8*). The analysis of the experimental data revealed that whereas the fast relaxation rate constants increased as a function of temperature, the slow reaction rate constants remained more or less constant. This is presumably because of a higher energy of activation of the slower relaxation rate constant. Figure 7 shows the Arrhenius plots for the octanoyl-CoA- and 3′-dephosphooctanoyl-CoA-dependent fast relaxation rate constants. The solid straight lines are the best fit of the experimental data according to the Arrhenius equation in the following format (eq 1).

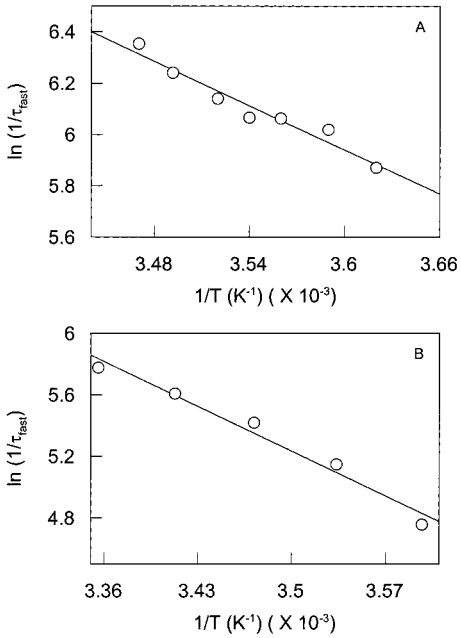


FIGURE 7: Arrhenius plots for the octanoyl-CoA- and 3′-dephosphooctanoyl-CoA-dependent reductive-half reaction with wild-type human liver MCAD. Panels A and B show the temperature dependence of the fast relaxation rate constant for the reaction of the wild-type enzyme with octanoyl-CoA and 3′-dephosphooctanoyl-CoA, respectively. The solid smooth line of panel A is the linear regression fit of the data for the activation energy ($E_a$) of 5.7 ± 0.6 kcal/mol and an intercept (ln *A*) of 16.3 ± 1.0. The corresponding parameters for the data of panel B were discerned to be 8.3 ± 0.8 kcal/mol and 19.8 ± 1.3, respectively.

$$\ln k = \ln A - \frac{E_a}{RT} \quad (1)$$

where *A*, $E_a$, *R*, and *T* represent the pre-exponential factor, the energy of activation, the universal gas constant, and the absolute temperature, respectively.

According to eq 1, the *Y*-axis intercept and slope serve as the measures of ln *A* and $E_a/R$, respectively. The $E_a$ values calculated for the octanoyl-CoA- and 3′-dephosphooctanoyl-CoA-dependent reductive half reactions were found to be 5.7 ± 0.6 and 8.3 ± 0.8 kcal/mol, respectively. It should be pointed out that the energy of activation for the octanoyl-CoA-dependent reaction, presented herein, is somewhat lower than that utilized (i.e., 6.9 kcal/mol) for predicting the rate constants at different temperatures in our previous publications (*6*, *8*). This discrepancy is presumably because, unlike our present determination, the earlier estimate was based on a limited number of experimental data points.

Given the energy of activation ($E_a$) for the octanoyl-CoA- and 3′-dephosphooctanoyl-CoA-dependent reductive half-reactions of the enzyme (Figure 7), the enthalpy of activation ($\Delta H^{\ddagger}$) for the above substrates can be determined ($\Delta H^{\ddagger} = E_a - RT$) to be 5.1 and 7.7 kcal/mol, respectively, at 25 °C.

Table 3: Changes in the Solvent-Accessible Surface Areas upon Binding of Ligands to Human Liver and Pig Liver MCADs and the Predicted $\Delta C_p^\circ$ Values[a]

| enzyme and/or ligand | $A_p$ (Å$^2$) | $A_{np}$ (Å$^2$) | $\Delta C_p^\circ$ (kcal mol$^{-1}$ K$^{-1}$) (*34*) | $\Delta C_p^\circ$ (kcal mol$^{-1}$ K$^{-1}$) (*35*) |
|---|---|---|---|---|
| PDB Code 1EGC | | | | |
| HMCAD (without ligand) | 9041 | 9495 | | |
| $C_8$-CoA | 551 | 514 | | |
| HMCAD−$C_8$-CoA | 8987 | 9200 | | |
| $\Delta A_p = -605$ Å$^2$, $\Delta A_{np} = -809$ Å$^2$ | | | | |
| predicted $\Delta C_p^\circ$'s for the binding of $C_8$-CoA to holo HMCAD | | | −0.17 | −0.21 |
| $dC_8$-CoA | 483 | 532 | | |
| HMCAD−$dC_8$-CoA | 8943 | 9221 | | |
| $\Delta A_p = -580$ Å$^2$,[b] $\Delta A_{np} = -806$ Å$^2$ | | | | |
| predicted $\Delta C_p^\circ$'s for the binding of $dC_8$-CoA to holo HMCAD | | | −0.18 | −0.21 |
| PDB Code 1EGD | | | | |
| HMCAD (apo structure) | 9617 | 9201 | | |
| $\Delta A_p = -1184$ Å$^2$,[c] $\Delta A_{np} = -513$ Å$^2$ | | | | |
| predicted $\Delta C_p^\circ$ for the binding of C8-CoA to apo HMCAD | | | −0.065 | 0.076 |
| PDB Code 3MDE | | | | |
| PMCAD (without ligand) | 9510 | 8485 | | |
| PMCAD−$C_8$-CoA | 9445 | 8251 | | |
| $\Delta A_p = -617$ Å$^2$, $\Delta A_{np} = -748$ Å$^2$ | | | | |
| predicted $\Delta C_p^\circ$ for the binding of C8-CoA to holo PMCAD | | | −0.15 | −0.18 |
| PDB Code 3MDD | | | | |
| PMCAD (apo structure) | 9094 | 8765 | | |
| $\Delta A_p = -201$ Å$^2$,[d] $\Delta A_{np} = -1028$ Å$^2$ | | | | |
| predicted $\Delta C_p^\circ$ for the binding of C8-CoA to apo PMCAD | | | −0.30 | −0.41 |

[a] HMCAD, PMCAD, $C_8$-CoA, and $dC_8$-CoA represent human liver MCAD, pig liver MCAD, octenoyl-CoA, and 3′-dephosphooctenoyl-CoA, respectively. Holo and apo structures represent the enzyme structures solved in the presence and absence of $C_8$-CoA. [b] Calculations were made after deleting the 3′-phosphate group from $C_8$-CoA, bound and free (i.e., unmerged) from the holo enzyme structure (1EGC). [c] Calculated by taking the values of $A_p$ and $A_{np}$ for unmerged $C_8$-CoA from the HMCAD holo structure (1EGC). The $A_p$ and $A_{np}$ values for HMCAD−$C_8$-CoA were taken directly from the calculations with 1EGC. [d] $A_p$ and $A_{np}$ values for PMCAD−$C_8$-CoA was taken from the calculations made with the holo structure (3MDE) of the enzyme.

From these values, it is apparent that the 3′-phosphate group contributes 2.6 kcal/mol in lowering the enthalpic barrier of activation ($\Delta\Delta H^\ddagger$) during the reductive half-reaction of the enzyme. Note that the latter value is comparable to 2.0 kcal/mol of enthalpic contribution of the 3′-phosphate group of octenoyl-CoA ($\Delta\Delta H^\circ$) in stabilizing the ground state of the enzyme−ligand complex (see above and the Discussion).

*Changes in the Solvent-Accessible Surface Areas upon Enzyme−Ligand Interactions.* It has been widely acknowledged that the heat capacity changes ($\Delta C_p^\circ$) for the binding of ligands to enzymes can be predicted on the basis of the changes in the solvent-accessible nonpolar and polar surface areas of the individual species (*34*−*37*). Given that the X-ray crystallographic structures of both pig liver and human liver enzymes in the absence and presence of $C_8$-CoA are known (*2*, *4*), we proceeded to determine the solvent-accessible nonpolar and polar surface areas of the individual enzymes, $C_8$-CoA, and the enzyme−$C_8$-CoA complexes according to the algorithm of Lee and Richards (*24*), via the ProState module of Homology-97 software. The sequence of steps involved during such calculations is described in detail in Materials and Methods. Table 3 summarizes the solvent-accessible nonpolar and polar surface areas of enzymes, ligands, and their complexes. From these data, we calculated the changes in the nonpolar ($\Delta A_{np}$) and polar ($\Delta A_p$) surface areas upon binding of $C_8$-CoA to both pig liver and human liver enzymes. It should be pointed out that since $\Delta A_{np}$ and $\Delta A_p$ are relative parameters, their magnitudes remain unaffected whether the above calculation is performed utilizing the individual subunit or the native enzyme tetramer. A casual perusal of the data of Table 3 reveals that the $\Delta A_{np}$ and $\Delta A_p$ values for the binding of $C_8$-CoA to the pig liver and human liver enzymes are −748 and −617 Å$^2$, and −809 and −605 Å$^2$, respectively.

We initially performed the above calculations utilizing the coordinates of the "holo" (i.e., $C_8$-CoA-bound) structures of both pig liver and human liver enzymes (see Materials and Methods). However, upon consideration that the above calculations may not be accurate since prior to binding of $C_8$-CoA, the above enzymes exist in their "apo" (i.e., in the absence of bound $C_8$-CoA) conformations, we decided to determine the magnitudes of $\Delta A_{np}$ and $\Delta A_p$, by calculating the surface areas of the corresponding "apo" enzymes, as well as those of holo enzymes and $C_8$-CoA. Such calculations allowed us to determine the magnitudes of $\Delta A_{np}$ and $\Delta A_p$ values for the binding of $C_8$-CoA to pig liver and human liver enzymes to be −1028 and −201 Å$^2$, and −513 and −1184 Å$^2$, respectively (Table 3). Note that the latter values are far different than those determined on the basis of the structural data of the holo enzymes alone. Furthermore, the $\Delta A_{np}$ and $\Delta A_p$ values for the binding of $C_8$-CoA to the pig liver enzyme are substantially different from those obtained for the binding of $C_8$-CoA to human liver enzymes.

We extended the above studies for the binding of 3′-dephospho-$C_8$-CoA to human liver MCAD. Prior to this calculation, the 3′-phosphate group of $C_8$-CoA was deleted, and the solvent-accessible surface areas of the energy-minimized structures of 3′-dephospho-$C_8$-CoA, enzyme, and the enzyme−3′-dephospho-$C_8$-CoA complex were determined as described above. The $\Delta A_{np}$ and $\Delta A_p$ values calculated for the binding of 3′-dephospho-$C_8$-CoA to the human liver enzyme were −806 and −580 Å$^2$, respectively (Table 3). A comparison of the latter values with those for the binding of $C_8$-CoA to the human liver enzyme reveals that $\Delta A_{np}$ remains practically invariant but $\Delta A_p$ increases by about 4% upon deletion of the 3′-phosphate group from $C_8$-CoA. Although the latter increase is not substantial, it is qualitatively suggestive of the fact that the relative hydrophobicity of $C_8$-CoA increases upon deletion of its 3′-phosphate group. This deduction is qualitatively corroborated by the fact that the deletion of the 3′-phosphate group results in a decrease in the experimentally determined $\Delta C_p^\circ$ value from −0.53 to −0.59 kcal mol$^{-1}$ K$^{-1}$ (see Figure 4). However, as we will describe in the Discussion, the experimentally determined $\Delta C_p^\circ$ values for the binding of octenoyl-CoA and 3′-dephosphooctenoyl-CoA to the human liver enzyme cannot be predicted on the basis of the X-ray crystallographic structures of apo and holo forms of either pig liver or human liver MCAD.

## DISCUSSION

The experimental data presented in the previous section lead to the following conclusions, related to the thermodynamic aspects of the ligand binding and catalysis in human

liver medium-chain acyl-CoA dehydrogenase (MCAD). (A) The binding energy of the 3′-phosphate group of $C_8$-CoA, in both the ground and transition states, is primarily contributed by the London−van der Waals interactions (involving the 3′-phosphate group of $C_8$-CoA and the surrounding protein moiety), and not by the putative hydrogen bonding between the amide oxygen (OD1) of Asn191 and one of the 3′-phosphate oxygen atoms (O7A2) of $C_8$-CoA (see Figure 1). (B) The enthalpic contribution of the 3′-phosphate group of octenoyl-CoA in the stabilization of the ground state ($\Delta\Delta H^\circ = -2.0$ kcal/mol) is similar to that involved in the stabilization of the transition state ($\Delta\Delta H^\ddagger = -2.6$ kcal/mol) during the octanoyl-CoA-dependent reductive half-reaction of the enzyme. (C) Both enthalpic ($\Delta H^\circ$) and heat capacity changes ($\Delta C_p^\circ$) for the binding of octenoyl-CoA to human liver MCAD are substantially more negative than those obtained with pig kidney MCAD. (D) The experimentally determined $\Delta C_p^\circ$ values for the binding of octenoyl-CoA and 3′-dephosphooctenoyl-CoA to human liver MCAD cannot be predicted on the basis of the changes in the solvent-accessible surface areas, determined from the X-ray crystallographic structures of pig liver and human liver enzymes, and enzyme−$C_8$-CoA complexes.

It should be mentioned that although the X-ray diffraction technique cannot detect hydrogen atoms, inter- and/or intramolecular hydrogen bondings are customarily assigned on the basis of the crystallographic data of protein−ligand complexes. Such assignments are based on the distances separating the potential hydrogen donor and hydrogen acceptor atoms. For example, given that the covalent and van der Waals contact radii of oxygen and hydrogen atoms are 0.30 and 0.66 Å, and 1.2 and 1.45 Å, respectively, an ideal (van der Waals contact) distance between two oxygen atoms (one as a hydrogen donor and the other as an acceptor) would be 3.61 Å (*38*). Any distance smaller than this (involving the hydrogen donor and acceptor oxygen atoms) can be attributed to the formation of a hydrogen bond. Hence, the bonding distance of 3.15 Å between OD1 of Asn191 and O7A2 of the 3′-phosphate group of $C_8$-CoA can be envisaged to be due to the formation of a hydrogen bond between the above residues.

Our goal of this investigation was to ascertain the energetic contribution of such a putative hydrogen bond during ligand binding and catalysis. The fact that the Asn191 → Ala mutation had no influence on either the $\Delta H^\circ$ or $\Delta G^\circ$ value for the binding of octenoyl-CoA to the enzyme led to the suggestion that the potential hydrogen bonding (between OD1 of Asn191 and O7A2 of $C_8$-CoA) had no functional role in stabilizing the ground-state structure of the enzyme−octenoyl-CoA complex. Neither did the above hydrogen bonding contribute to stabilizing the transition-state structure during the octanoyl-CoA-dependent reductive half-reaction of the enzyme. On the other hand, the deletion of the 3′-phosphate group influenced both thermodynamic parameters (i.e., $\Delta G^\circ$ and $\Delta H^\circ$) for the binding of octenoyl-CoA to the enzyme, and the steady-state and transient kinetic parameters for the octanoyl-CoA-dependent reaction. Clearly, the energetic contribution of the 3′-phosphate group of $C_8$-CoA is not identical to that given by the substitution of Asn191 → Ala at the enzyme site.

In attempting to discern the molecular basis of the above effects, we note that the strength of hydrogen bonds is dependent on the distance separating the donor and acceptor atoms, spatial relationships between OH (donor) and O (acceptor) atoms, and their microenvironments (*39*−*41*). In nonpolar solvents, the hydrogen bond energy has been estimated to fall in the range of −3 to −10 kcal/mol (*40*, *41*). In aqueous solution, the strength of a hydrogen bond is dependent on the preferential interaction of the water molecules with the donor, the acceptor, and the hydrogen-bonded (donor−acceptor complex) species. Fersht (*56*) argues that the hydrogen bond formation between an enzyme and a substrate site is a result of the following exchange reaction (eq 2).

$$\text{E}\cdots\text{HOH} + \text{S}\cdots\text{HOH} \rightleftharpoons \text{E}\cdots\text{S} + \text{HOH}\cdots\text{HOH} \quad (2)$$

In eq 2, the water molecules, involved in the initial hydrogen bonds at enzyme and substrate sites, are released to the bulk phase, leading to the hydrogen-bonded enzyme−substrate species. Under normal conditions (i.e., in the absence of any geometric constraints), if the hydrogen bonding between an enzyme and a substrate site involves electronically similar (and uncharged) donor and acceptor groups (e.g., O), the overall exchange reaction of eq 2 would be isoenthalpic. In this case, the hydrogen bond formation would be entropically favored due to the release of the enzyme and substrate-bound water molecules in the bulk phase. The energetic contribution ($\Delta G^\circ$) of such a hydrogen bond has been estimated to be in the range of 0.5−1.8 kcal/mol (*56*). If the enzyme site is mutated such that it no longer forms a hydrogen bond with the water molecule, the above-noted entropic advantage would be impaired, resulting in a loss of binding energy by the above magnitude (*56*). Obviously, some variation in the above estimate may occur if the donor and acceptor groups are charged species, and/or if the intervening water structure is altered. However, irrespective of the case, if OD1 of Asn191 formed a hydrogen bond with O7A2 of the 3′-phosphate group of $C_8$-CoA, both $\Delta G^\circ$ and $\Delta H^\circ$ values for the binding of octenoyl-CoA to the wild-type enzyme would not be equal to the corresponding values for the binding of octenoyl-CoA to the N191A mutant enzyme. Since the above values exhibit a marked similarity, it is evident that the structurally predictable hydrogen bond between OD1 of Asn191 and O7A2 of the 3′-phosphate of $C_8$-CoA either is nonexistent or has a miniscule (undetectable) energetic contribution.

Figure 8 shows the water-accessible surface areas (Connolly surface; *42*) within a 4 Å perimeter of the enzyme-bound $C_8$-CoA and 3′-dephospho-$C_8$-CoA (Figure 8). Note that a major part of the $C_8$-CoA molecule (including the 3′-phosphate group) and the side chain of Asn191 are solvated by the water molecules. If such water molecules are structured in the vicinity of the 3′-phosphate group as if they are in the bulk phase, the binding energy of the 3′-phosphate group of $C_8$-CoA would remain the same, irrespective of whether Asn191 or Ala191 was present at the enzyme site. Although this is the most plausible explanation of our experimental data, we are hesitant to rule out, at this time, other thermodynamic possibilities.

The deletion of the 3′-phosphate group from octenoyl-CoA is likely to alter the energetic contribution of the ligand due to changes in solvation, geometric configuration, and London−van der Waals forces involving the protein struc-

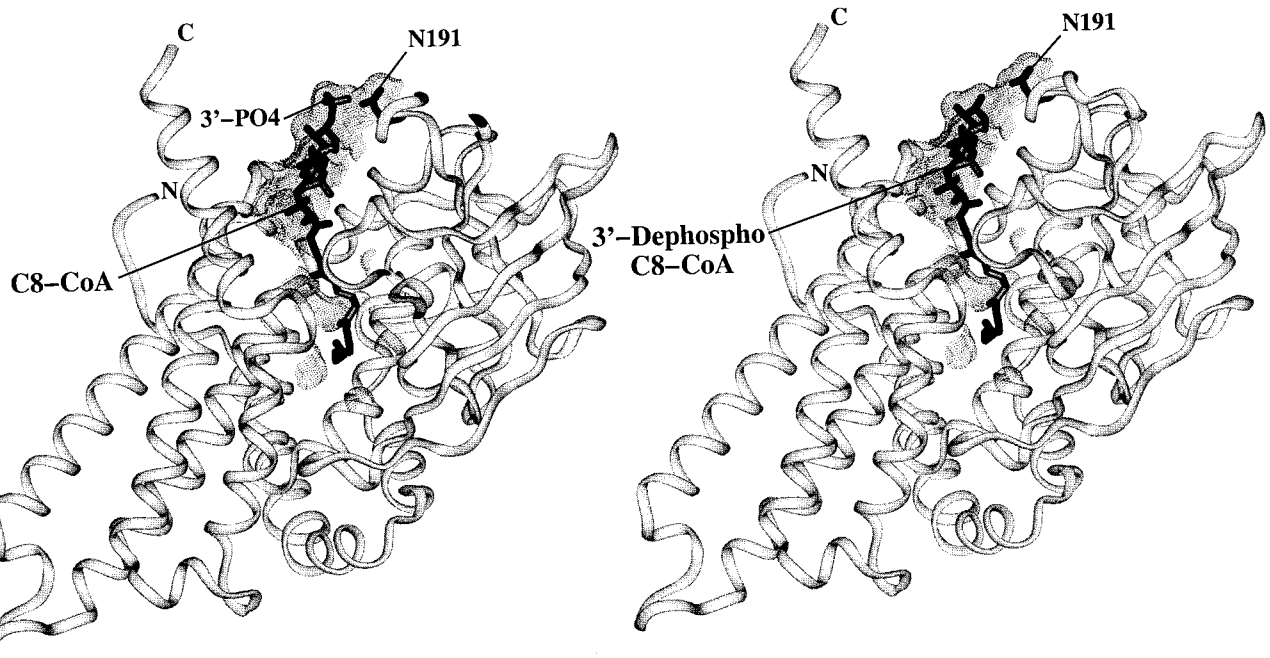


FIGURE 8: Water-accessible surface areas (Connolly surface) within 4 Å of $C_8$-CoA (left) and 3′-dephospho-$C_8$-CoA (right) bound to human liver MCAD.

ture. Of these, as described below, the deletion of the 3′-phosphate group from $C_8$-CoA hardly affects (≤3%) the predicted $\Delta C_p°$ value for the binding of the ligand to the enzyme. Hence, the enthalpic contribution due to solvation and/or desolvation of the 3′-phosphate group is negligible. Working from the assumption that the deletion of the 3′-phosphate group from $C_8$-CoA does not substantially contribute to changes in the configurational energy, we propose that the experimentally determined enthalpic and free energy contributions of the 3′-phosphate group of $C_8$-CoA are due to the London−van der Waals interactions.

In a series of communications (*5*−*8*, *19*), we demonstrated that the microscopic pathways for the binding of octenoyl-CoA to (both pig kidney and human liver) MCAD and the octanoyl-CoA-dependent reductive half-reaction are precisely the same. Both these processes occur via two steps, with equal magnitudes for the rate and equilibrium constants (*5*−*7*). We proposed that the origin of the above similarity must be due to an intimate coupling between the protein conformational change and the ligand structural changes (*6*, *7*). In light of these facts, it follows that the thermodynamic parameters derived for the octanoyl-CoA-dependent reaction can be applied to the octenoyl-CoA-dependent binding process, and vice versa. If it is assumed that the contribution of the 3′-phosphate group is equal for both octanoyl-CoA- and octenoyl-CoA-dependent processes, the $\Delta\Delta H°$ derived from the microcalorimetric titration results (see Figures 2 and 3A) can be taken as a qualitative measure of the effect of the 3′-phosphate group in stabilization of the ground-state structure of octanoyl-CoA during the reductive half-reaction of the enzyme. Since $\Delta\Delta H°$ (−2.0 kcal/mol) is not too different from $\Delta\Delta H^{‡}$ (−2.6 kcal/mol), it appears plausible that the enthalpic contribution of the 3′-phosphate group is more or less the same in stabilization of both ground and transition states during the octanoyl-CoA-dependent reaction.

On the basis of numerical simulations and model building studies (*6*), we proposed that the fast relaxation rate constant ($1/\tau_{fast}$) of the octanoyl-CoA reductive half-reaction is given by the sum of the forward and reverse rate constants (i.e., $1/\tau_{fast} = k_f + k_r$, and $k_f = k_r$). If it is assumed that the above relationship remains the same at all temperatures, the rate constant for the forward step for the octanoyl-CoA- and 3′-dephosphooctanoyl-CoA-dependent reductive half-reaction (at 25 °C) can be calculated to be 383 and 171 $s^{-1}$, respectively. From these rate constants, the free energy of activation ($\Delta G^{‡}$) for the forward step of the reductive half-reaction can be calculated according to the following relationship (eq 3).

$$\Delta G^{‡} = -RT \ln\left(\frac{k_f h}{k_B T}\right) \tag{3}$$

where $R$ is the gas constant (8.31 J $K^{-1}$ $mol^{-1}$), $T$ is the absolute temperature, $k_f$ is the forward rate constant, $h$ is Plank's constant ($6.63 \times 10^{-34}$ J s), and $k_B$ is Boltzmann's constant ($1.38 \times 10^{-23}$ J $K^{-1}$). The calculated $\Delta G^{‡}$ values for the octanoyl-CoA and 3′-dephosphooctanoyl-CoA dependent reactions were found to be 13.9 and 14.4 kcal/mol at 25 °C, respectively. Hence, the free energy contribution of the 3′-phosphate group in stabilizing the transition state during the reductive half-reaction ($\Delta\Delta G^{‡}$) is 0.5 kcal/mol. Note that the latter value is somewhat lower than the $\Delta\Delta G°$ (−1.2 kcal/mol at 25 °C) obtained for the contribution of the 3′-phosphate group in stabilization of the ground state. Hence, it appears to be evident that the entropic contribution of the 3′-phosphate group is different in the ground and transition states. It should be mentioned that the energetic contribution of the 3′-phosphate group of the $C_8$-CoA-dependent reaction of MCAD (presented herein) is somewhat different from that obtained for the myristoyl-CoA-dependent reaction of myristoyl-CoA:protein *N*-myristoyltransferase (*49*).

*Relationship between $\Delta C_p°$ and the Solvent-Accessible Surface Areas.* It should be emphasized that the $\Delta C_p°$ value determined for the binding of octenoyl-CoA to pig kidney MCAD (−0.37 ± 0.05 kcal $mol^{-1}$ $K^{-1}$; *13*) is substantially

different from that determined for the binding of octenoyl-CoA to human liver MCAD ($\Delta C_p^\circ = -0.53 \pm 0.03$ kcal mol$^{-1}$ K$^{-1}$; Figure 4). Since in these studies, octenoyl-CoA served as a common ligand, the above-noted difference in the $\Delta C_p^\circ$ value must originate from a difference in the protein structures of pig kidney and recombinant human liver MCADs. Such an inference would appear to be surprising in light of the fact that there is a marked amino acid sequence homology among MCADs of different biological origins (*52*), and that the X-ray crystallographic structures of the (native) pig liver and (recombinant) human liver enzymes are indistinguishable (*2*, *4*). Although no structural information about pig kidney MCAD is yet available, it is widely conceived that the structure of the pig kidney enzyme would be more or less the same as those of pig liver and human liver enzymes.

On the basis of the thermodynamic measurements of the partitioning of various compounds between polar and nonpolar phases and protein unfolding, as well as binding of selected ligands to their cognate proteins, it has been argued that the origin of $\Delta C_p^\circ$ lies in the exposure and/or burial of nonpolar surface areas to or from the aqueous phase (*26*−*31*, *34*−*37*). Hence, for protein−ligand complexes, whose three-dimensional structures are known to atomic resolutions, $\Delta C_p^\circ$ could be predicted on the basis of the solvent-accessible surface areas. In recent years, several empirical relationships for predicting the $\Delta C_p^\circ$ values on the basis of changes in the solvent-accessible polar and nonpolar surface areas upon protein−ligand interactions have been proposed (*34*, *35*). A generalized form of such a relationship is given by eq 4.

$$\Delta C_p = C_{p,\mathrm{p}} \Delta A_\mathrm{p} + C_{p,\mathrm{np}} \Delta A_\mathrm{np} \qquad (4)$$

where $\Delta A_\mathrm{p}$ and $\Delta A_\mathrm{np}$ refer to the combined changes in the polar and nonpolar solvent-accessible surface areas, respectively, of proteins and ligands upon their interactions. $C_{p,\mathrm{p}}$ and $C_{p,\mathrm{np}}$ are the heat capacity functions for changes in the polar and nonpolar surface areas, respectively. The magnitudes of $C_{p,\mathrm{p}}$ and $C_{p,\mathrm{np}}$ have been proposed to be −0.14 and 0.32 cal mol$^{-1}$ K$^{-1}$ Å$^{-2}$, respectively, by Spolar et al. (*34*), and −0.26 and 0.45 cal mol$^{-1}$ K$^{-1}$ Å$^{-2}$, respectively, by Murphy et al. (*35*).

If the changes in the solvent-accessible surface areas of human liver MCAD and $C_8$-CoA upon their interactions are taken into account (Table 3), $\Delta C_p^\circ$ was predicted to be −0.17 and −0.21 kcal mol$^{-1}$ K$^{-1}$ according to Spolar et al. (*34*) and Murphy et al. (*35*), respectively. Note that these values are about 3 times less negative than those determined experimentally. When the above prediction was made for the binding of 3′-dephosphooctenoyl-CoA, $\Delta C_p^\circ$ values were found to be −0.18 and −0.21 kcal mol$^{-1}$ K$^{-1}$, respectively. Although the latter values are slightly (about 2%) more negative (as expected for a relative increase in the hydrophobicity of $C_8$-CoA upon deletion of its 3′-phosphate group), they are considerably less negative than those observed experimentally.

Table 3 summarizes the magnitudes of $\Delta C_p^\circ$ values, predicted on the basis of the changes in the solvent-accessible polar and nonpolar surface areas of the interacting components, utilizing both pig liver and human liver MCAD structures in the absence (apo) and presence (holo) of $C_8$-CoA. The former structures of both pig and human liver enzymes were utilized considering that prior to binding of the ligands, the enzymes predominated in their apo conformations. As is evident from the data of Table 3, the solvent-accessible surface areas calculated from the apo enzyme structures are considerably different from those obtained from the corresponding holo structures. Hence, the $\Delta C_p^\circ$ value predicted by taking into account both apo and holo structures yielded results different from that predicted from the holo structure alone. Likewise, the predictions made using the structural coordinates of pig liver (apo and holo) enzymes yielded different results. We also performed the above calculations in the absence and presence of the crystallographic water molecules, as well as utilizing tetrameric forms of both human liver and pig liver enzymes (data not shown), and found no situation where the predicted values would match (within the ±5−10% range) the experimentally determined values. It should be pointed out that the above disparity is not dependent on the empirically derived $C_\mathrm{p}$ and $C_\mathrm{np}$ values utilized in these calculations. Any values chosen for these parameters would yield more or less similar predictions under one situation or the other. A cumulative account of these comparisons leads to the suggestion that the experimentally determined $\Delta C_p^\circ$ values (for the binding of $C_8$-CoA and 3′-dephospho-$C_8$-CoA to human liver MCAD) cannot be quantitatively predicted on the basis of the X-ray crystallographic data.

The following question arises. Unlike those of other protein−ligand systems (*53*−*55*), why can the $\Delta C_p^\circ$ values for the binding of octenoyl-CoA and 3′-dephosphooctenoyl-CoA to human liver MCAD not be predicted on the basis of the changes in the solvent-accessible polar and nonpolar surface areas? In this context, it has been argued the above predictions fail if the proteins undergo conformational changes upon binding with their ligands (*53*). Such an argument is based on the assumption that the protein conformational changes alter the solvent accessibility of the enzyme site environments. Unfortunately, this does not appear to be the case for pig liver and human liver MCADs; both these enzymes undergo negligible conformational changes upon interaction with $C_8$-CoA. This prompts consideration that solvent accessibility is not the exclusive determinant of the experimentally derived $\Delta C_p^\circ$ values, and thus, some other physical factors might be responsible for the above-noted discrepancies in the $\Delta C_p^\circ$ values. It should be mentioned that several other investigators have arrived at the same conclusion with other protein−ligand systems (*45*−*48*).

In their investigation with the *try* repressor/operator system, Ladbury et al. (*48*) concluded that a part of the experimentally derived $\Delta C_p^\circ$ is contributed by the formation of specific macromolecular interfaces. According to these authors, a highly complementary or specific interaction between a protein and ligand gives rise to a large negative $\Delta C_p^\circ$ value. In light of this hypothesis, the surface complementarity between octenoyl-CoA and human liver MCAD must be higher than that between pig kidney MCAD and octenoyl-CoA, and such a physical determinant may be responsible for a 0.16 kcal mol$^{-1}$ K$^{-1}$ more negative $\Delta C_p^\circ$ value. This is not unexpected given that the $\Delta H^\circ$ values for the binding of both octenoyl-CoA and IACoA to the human liver enzyme are 7−14 kcal/mol more negative than those obtained with the pig kidney enzyme (*13*, *14*, *25*). The

above explanation is consistent with Sturtevant's view (*50*) that the binding of ligands to proteins freezes several ("soft") vibrational modes, which are responsible for $\Delta C_p^\circ$ values more negative than those predicted on the basis of the solvent accessibility. Hence, our inability to predict the experimentally determined $\Delta C_p^\circ$'s (for the binding of octenoyl-CoA and 3′-dephosphooctenoyl-CoA to human liver MCAD), as well as the discrepancy between the $\Delta C_p^\circ$ values for the binding of octenoyl-CoA to human liver versus pig kidney enzyme, may have a common physical determinant.

In light of the above discussion, it is obvious that irrespective of the nature of the physical forces, which give rise to the experimentally determinable $\Delta C_p^\circ$ values, they cannot be conceived on examination of the X-ray crystallographic structures of the enzyme−ligand complexes. A qualitatively similar situation prevails while we attempt to explain our transient kinetic data for the binding of a variety of ligands to both pig kidney and human liver enzymes, as well as the transient courses of the enzyme catalyses (*1*, *5*−*11*, *15*−*19*). All these experimental data demand an obligatory change in the protein conformation, but there is hardly any crystallographic evidence to support them. These puzzling outcomes imply that either the protein structure of MCAD creates an active site cavity, like a "static cage", at which ligand binding and catalysis occur without affecting its structure, or structural changes are so minute and/or subtle that they are not discerned in the crystallographic data of contemporary resolutions (e.g., 2.4 Å). Of these, the latter possibility is highly important in the rationalization of a wealth of spectroscopic, kinetic, and thermodynamic data on this enzyme (*1*, *5*−*11*, *15*−*19*, *52*). We believe small changes in the structure of MCAD (and possibly in other enzymes) may just be adequate to lead to large differences in their functional (i.e., spectroscopic, kinetic, and thermodynamic) properties during ligand binding and catalysis. For example, we have recently demonstrated that the spectroscopic, thermodynamic, and kinetic properties for the binding of acetoacetyl-CoA and IACoA are drastically affected (albeit in the opposite direction) upon mutation of an active site residue, Glu376 to Asp (*25*). Whereas the above mutation increases the $\Delta H^\circ$ value for the binding of acetoacetyl-CoA by 5.6 kcal/mol, it decreases the $\Delta H^\circ$ value for the binding of IACoA by 6.4 kcal/mol. The model building studies for the interaction of these ligands with the wild-type and mutant enzymes suggest that the above thermodynamic changes are manifested by minute changes ($\leq$0.35 Å) in the distance separating the enzyme-bound CoA ligands and FAD. The generality or frequency of such occurrences during enzyme−ligand interactions and enzyme catalysis must await further studies.

## REFERENCES


1. Srivastava, D. K., Kumar, N. R., and Peterson, K. L. (1995) *Biochemistry 34*, 4625−4632.
2. Kim, J.-J. P., Wang, M., and Paschke, R. (1993) *Proc. Natl. Acad. Sci. U.S.A. 90*, 7523−7527.
3. Kelly, D. P., Kim, J.-J. P., Billadello, J. J., Hainline, B. E., Chu, T. W., and Strauss, A. W. (1987) *Proc. Natl. Acad. Sci. U.S.A. 84*, 4068−4072.
4. Lee, H.-J. K., Wang, M., Paschke, R., Nandy, A., Ghisla, S., and Kim, J.-J. P. (1996) *Biochemistry 35*, 12412−12420.
5. Kumar, N. R., and Srivastava, D. K. (1994) *Biochemistry 33*, 8833−8841.
6. Kumar, N. R., and Srivastava, D. K. (1995) *Biochemistry 34*, 9434−9443.
7. Peterson, K. L., Sergienko, E. E., Wu, Y., Kumar, N. R., Strauss, A. W., Oleson, A. E., Muhonen, W. W., Shabb, J. B., and Srivastava, D. K. (1995) *Biochemistry 34*, 14942−14953.
8. Peterson, K. L., and Srivastava, D. K. (1997) *Biochem. J. 325*, 751−760.
9. Kumar, N. R., Peterson, K. L., and Srivastava, D. K. (1996) *Flavin and Flavoproteins* (Stevenson, K. J., Massey, V., and Williams, C. W., Eds.) pp 633−636, University of Calgary Press, Calgary, Canada.
10. Johnson, J. K., and Srivastava, D. K. (1993) *Biochemistry 32*, 8004−8013.
11. Johnson, J. K., Kumar, N. R., and Srivastava, D. K., (1994) *Biochemistry 33*, 4738−4744.
12. Schopfer, L. M., Massey, V., Ghisla, S., and Thorpe, C. (1988) *Biochemistry 27*, 6599−6611.
13. Srivastava, D. K., Wang, S., and Peterson, K. L. (1997) *Biochemistry 36*, 6359−6366.
14. Qin, L., and Srivastava, D. K. (1998) *Biochemistry 37*, 3499−3508.
15. Johnson, J. K. (1994) Ph.D. Dissertation, North Dakota State University, Fargo, ND.
16. Johnson, J. K., Wang, Z. X., and Srivastava, D. K. (1992) *Biochemistry 31*, 10564−10575.
17. Johnson, J. K., Kumar, N. R., and Srivastava, D. K. (1993) *Biochemistry 32*, 11575−11585.
18. Srivastava, D. K., Johnson, J. K., Kumar, N. R., and Peterson, K. L. (1996) *Flavins and Flavoproteins* (Stevensen, K. J., Massey, V., and Williams, C. W., Eds.) pp 641−644, University of Calgary Press, Calgary, Canada.
19. Peterson, K. L., Galitz, D. S., and Srivastava, D. K. (1998) *Biochemistry 37*, 1697−1705.
20. Lehman, T. C., Hale, D. E., Bhala, A., and Thorpe, C. (1990) *Anal. Biochem. 186*, 280−284.
21. Thorpe, C., Matthews, R. G., and Williams, C. W., Jr. (1979) *Biochemistry 18*, 331−337.
22. Bernert, J. T., and Sprecher, H. (1977) *J. Biol. Chem. 252*, 6737−6744.
23. Wiseman, T., Williston, S., Brandt, J. F., and Lin, L.-N. (1989) *Anal. Biochem. 17*, 131−137.
24. Lee, B., and Richards, F. M. (1971) *J. Mol. Biol. 55*, 379−400.
25. Srivastava, D. K., and Peterson, D. K. (1998) *Biochemistry 37*, 8446−8456.
26. Edsall, J. T. (1935) *J. Am. Chem. Soc. 57*, 1506−1507.
27. Tanford, C. (1980) *The Hydrophobic Effect*, 2nd ed., Wiley, New York.
28. Baldwin, R. L. (1986) *Proc. Natl. Acad. Sci. U.S.A. 83*, 8069−8072.
29. Spolar, R. S., Ha, J.-H., and Record, M. T., Jr. (1989) *Proc. Natl. Acad. Sci. U.S.A. 86*, 8382−8385.
30. Privalov, P. L. (1979) *Adv. Protein Chem. 33*, 167−241.
31. Murphy, K. P., Privalov, P. L., and Gill, S. J. (1989) *Science 247*, 559−561.
32. Hackney, D. D. (1990) in *The Enzymes* (Sigman, D. S., and Boyer, P. D., Eds.) 3rd ed., Vol. 19, pp 1−36, Academic Press, San Diego, CA.
33. Burbaum, J. J., Raines, R. T., Albery, W. J., and Knowles, J. R. (1989) *Biochemistry 28*, 9293−9305.
34. Spolar, R. S., Livingstone, J. R., and Record, M. T., Jr. (1992) *Biochemistry 31*, 3947−3955.
35. Murphy, K. P., Xie, D., Garcia, K. C., Amzel, L. M., and Freire, E. (1993) *Proteins 15*, 113−120.
36. Makhatadze, G. I., and Privalov, P. L. (1990) *J. Mol. Biol. 213*, 375−384.
37. Makhatadze, G. I., and Privalov, P. L. (1993) *J. Mol. Biol. 232*, 639−659.
38. Pauling, L. (1945) *The Nature of the Chemical Bond*, Cornell University Press, New York.
39. Jeffrey, G. A. (1992) *Adv. Enzymol. Relat. Areas Mol. Biol. 65*, 217−254.
40. Fersht, A. (1985) *Enzyme Structure and Mechanism*, Freeman and Co., New York.

41. Jencks, W. P. (1987) *Catalysis in Chemistry and Enzymology*, Dover Publications, Inc., New York.
42. Connolly, M. L. (1983) *Science 221*, 709−713.
43. Kieweg, V., Krautle, F.-G., Nandy, A., Engst, S., Vock, P., Abdel-Ghany, A.-G., Bross, P., Gregersen, N., Rasched, I., Strauss, A., and Ghisla, S. (1997) *Eur. J. Biochem. 246*, 548−556.
44. Macheroux, P., Sanner, C., Buttner, H., Kieweg, V., Ruterjans, H., and Ghisla, S. (1997) *J. Biol. Chem. 378*, 1381−1385.
45. Holdgate, G. A., Tunnicliffe, A., Ward, W. H. J., Weston, S. A., Rosenbrock, G., Barth, P. T., Taylor, I. W. F., Pauptit, R. A., and Timms, D. (1997) *Biochemistry 36*, 9663−9673.
46. Rowe, E. S., Zhang, F., Leung, T. W., Parr, J. S., and Guy, P. T. (1998) *Biochemistry 37*, 2430−2440.
47. Raman, C. S., Allen, M. J., and Nall, B. T. (1995) *Biochemistry 34*, 5831−5838.
48. Ladbury, J. E., Wright, J. G., Sturtevant, J. M., and Sigler, P. B. (1994) *J. Mol. Biol. 238*, 669−681.
49. Bhatnagar, R. S., Jackson-Machelski, E., McWherter, C. A., and Gordon, J. L. (1994) *J. Biol. Chem. 269*, 11045−11053.
50. Sturtevant, J. M. (1977) *Proc. Natl. Acad. Sci. U.S.A. 74*, 2236−2240.
51. Frerman, F. E., Miziorko, H. M., and Beckman, J. D. (1980) *J. Biol. Chem. 255*, 11192−11198.
52. Engel, P. C. (1990) in *Chemistry and Biochemistry of Flavoenzymes* (Muller, F., Ed.) Vol. 3, pp 597−655, CRC Press, Boca Raton, FL.
53. Spolar, R. S., and Record, T., Jr. (1994) *Science 263*, 777−784.
54. Murphy, K. P., and Freire, E. (1992) *Adv. Protein Chem. 43*, 313−361.
55. Faergeman, N. J., Sigurskjold, B. W., Kragelund, B. B., Andersen, K. V., and Knudsen, J. (1996) *Biochemistry 35*, 14118−14126.
56. Fersht, A. R. (1987) *Trends Biochem. Sci. 12*, 301−304.

BI980949M